Hindawi
Journal of Nanomaterials
Volume 2022, Article ID 2485291, 10 pages
https://doi.org/10.1155/2022/2485291

Research Article

Facile Ultrasound-Assisted Green Synthesis of NiO/Chitosan Nanocomposite from Mangosteen Peel Extracts as Antibacterial Agents

Thi Mai Huong Pham,[1] Ngoc Son Nguyen,[2] The Nam Dao,[2] Thu Thuy Le,[3] Thi Hanh Nguyen,[4] Ha Ngan Pham,[4] and Thi Huong Nguyen[2]

[1]*Hanoi University of Industry, Hanoi 100000, Vietnam*
[2]*Institute of Chemistry and Material, Hanoi 100000, Vietnam*
[3]*Hanoi University of Natural Resources and Environment, Hanoi 100000, Vietnam*
[4]*VNU University of Science, Hanoi 100000, Vietnam*

Correspondence should be addressed to Thi Huong Nguyen; nguyenhuong0916@gmail.com

Received 15 March 2022; Accepted 23 May 2022; Published 10 June 2022

Academic Editor: Haisheng Qian

Copyright © 2022 Thi Mai Huong Pham et al. This is an open access article distributed under the Creative Commons Attribution License, which permits unrestricted use, distribution, and reproduction in any medium, provided the original work is properly cited.

In this study, NiO/chitosan (NiO/CS) nanocomposite was synthesized via a green method in which nickel nitrate hexahydrate as a precursor and mangosteen (*Garcinia mangostana* L.) peel extract as a reducing agent using an ultrasound-assisted coprecipitation method. The NiO/CS nanoparticles were characterized by X-ray diffraction, Fourier-transform infrared (FTIR) spectroscopy, transmission electron microscopy, and dynamic light scattering. NiO/CS nanocomposite had a cubic spinel structure and contained NiO nanoparticles with good crystallinity. The appearance of the Ni–O band at 465 cm^{-1} in the FTIR spectrum confirmed the formation of NiO. The NiO/CS nanocomposite sizes ranged from 14–30 nm with an average particle size of 28 nm. Magnetic characterization results show that the saturation magnetism is quite high, contributing to NiO/CS being available in many applications. The antibacterial efficacy of NiO/CS nanocomposites was tested against *Saccharomyces cerevisiae* along with Gram-positive (*Bacillus subtilis*) and Gram-negative (*Escherichia coli*) bacteria using the disc diffusion method and determined the minimum inhibitory concentration (MIC).

1. Introduction

Metal oxide nanoparticles (NPs) with various properties are used in applications such as photocatalysis [1], lithium-ion batteries [2], antimicrobial materials [3, 4], magnetic and antibacterial materials [3], sensors [5], and thermally conductive and antiferromagnetic films [6]. Because of their peculiar physicochemical properties, NPs have different thermal, optical, electrical, and mechanical properties compared to their larger counterparts [7, 8]. Coprecipitation, sol-gel, electrospray synthesis, laser ablation, and hydrothermal methods [9–11] have been developed for the synthesis of nanomaterials. Biosynthesis has attracted attention because it takes advantage of nonhazardous and environmentally friendly biological systems such as bacteria [12], fungi [13], leaves [14, 15], vitamins [16], and yeast to synthesize NPs of metal oxide.

In the present work, NiO/chitosan (NiO/CS) nanomaterials were prepared by a novel process based on mangosteen peel extract (Garcinia mangostana L.) as a reducing agent and stabilizing agent with the help of ultrasonic waves. The synthetic process involved two stages: the synthesis of NiO NPs from G. mangostana L. peel using an ultrasound-assisted coprecipitation method and the synthesis of NiO/CS nanocomposites.

Karthiga et al. successfully used mangosteen peel extract in the rapid and simple synthesis of uniform, monodisperse, spherical, and crystalline silver NPs with an average particle size of 30 nm [17]. Aminuzzaman et al. used the aqueous extract of the G. mangostana fruit peel as a reducing agent

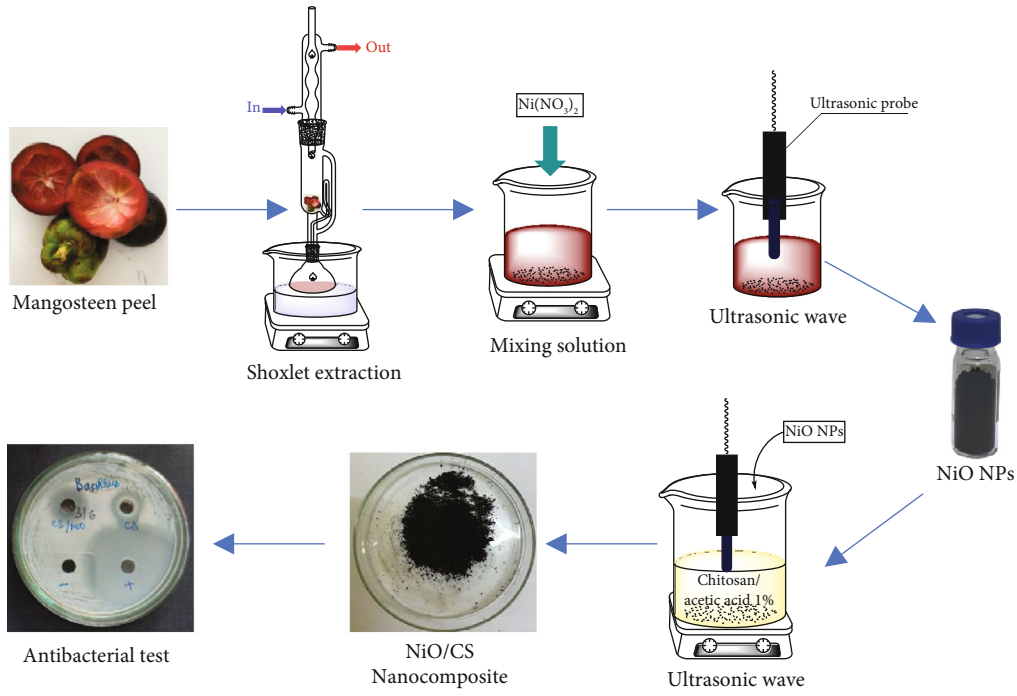


Figure 1: Schematic showing the synthesis of the NiO/CS nanocomposite.

and stabilizer to synthesize ZnO NPs. The obtained ZnO NPs are spherical in shape, with an average diameter of 21 nm, and have photocatalytic activity in the degradation of malachite green dye [18]. G. mangostana, commonly known as mangosteen, is a tropical fruit tree commonly grown in Southeast Asia. The ripe fruit has a thick outer skin with a deep purple-red color. The mangosteen fruit contains phenolic compounds such as tannins, flavonoids, xanthones, and other bioactive substances [19]. Mangosteen peel extract has been reported to have good antioxidant and bactericidal properties [20–23]. Mangosteen peel extract can reduce metal-oxide NPs and stabilize NPs, providing control over the particle shape and size [17, 18].

Chitosan is a biofilm-forming agent that contains positively charged glucosamines that interact with negatively charged phospholipid components of bacterial membranes. This increases the permeability of the bacterial membrane and causes leakage of the cytoplasm, leading to cell death. In addition, chitosan is also believed to have the ability to promote the production of active oxygen free radicals that cause cell death [24].

The antibacterial activity of chitosan is determined by several factors such as chitosan type, molecular weight, pH, and solvent [25, 26]. Thus, the combination of chitosan and NiO NPs into a NiO/CS nanocomposite is expected to produce an antibacterial material with multifunctional properties [1, 3, 9]. Nonconventional ultrasound-based methods have been described as successful and ecologically inviting strategies for chemical modification of polymers with various applications. For example, Bhatt et al. detailed the manufacture of a NiO/CS nanocomposite beneath ultrasonic radiation; the NiO/CS nanocomposite appears potentially as a dielectric fabric [9]. Ultrasound-assisted methods have also been applied to prepare NiO nanospheres for supercapacitors [27] and NiO/Ag_3VO_4 nanocomposites for visible-light photocatalysis and antibacterial applications [28]. Similarly, Raja used a sonochemical route to prepare NiO/Ag_3VO_4 ternary nanocomposites with advantages in photodegradation of organic compounds and antibacterial activity compared to conventionally prepared materials [28]. However, to the leading of our information, NiO/CS NPs with antibacterial and antifungal properties have not been prepared by utilizing an ultrasound-assisted coprecipitation method.

In this study, NiO/CS nanocomposite was synthesized by ultrasonic coprecipitation with nickel nitrate hexahydrate precursor and mangosteen (*G. mangostana* L.) peel extract as reducing and stabilizing agents. The antibacterial activity, as well as the effect of the chitosan content, was examined.

2. Experimental

2.1. Materials. Nickel (II) nitrate hexahydrate ($Ni(NO_3)_2$•$6H_2O$) and acetic acid (glacial) were purchased from Merck. The NH_3 solution and ethanol were provided by Macklin-China. Chitosan (CS: 100-200 mPa·s) was obtained from Aladin, China. The raw mangosteen peel was collected from Southern Vietnam, and deionized water was used throughout the study.

Mangosteen peel was washed with deionized water, chopped into small pieces, and dried at 60°C. The extract was prepared by heating 6 g of the dried peel with 100 ml of ethanol/water (1 : 2, *v*/*v*) at 80°C for 60 min in an Erlenmeyer flask. The extract was then cooled to room temperature, filtered the residue out, and stored at 6-8°C for use within a week.

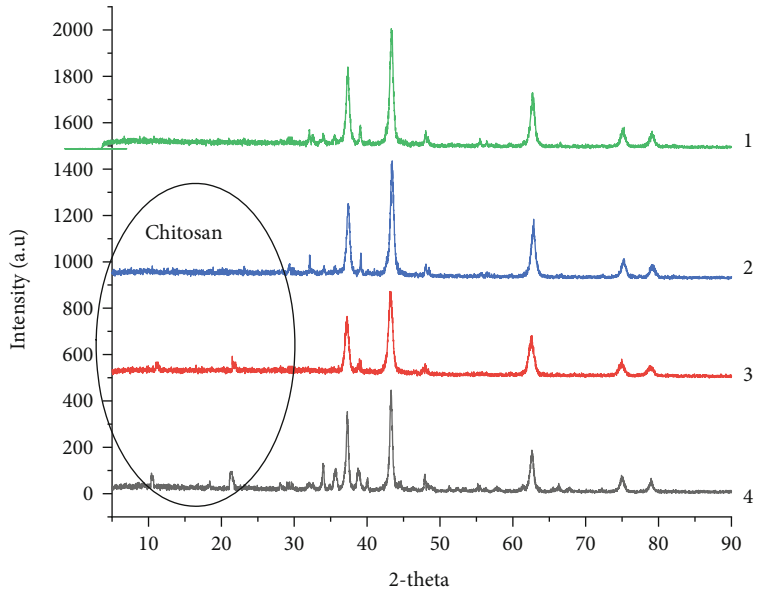


Figure 2: XRD patterns of NiO NPs (1) and NiO/CS nanocomposites with different chitosan content: (2) 5%, (3) 10%, and (4) 20%.

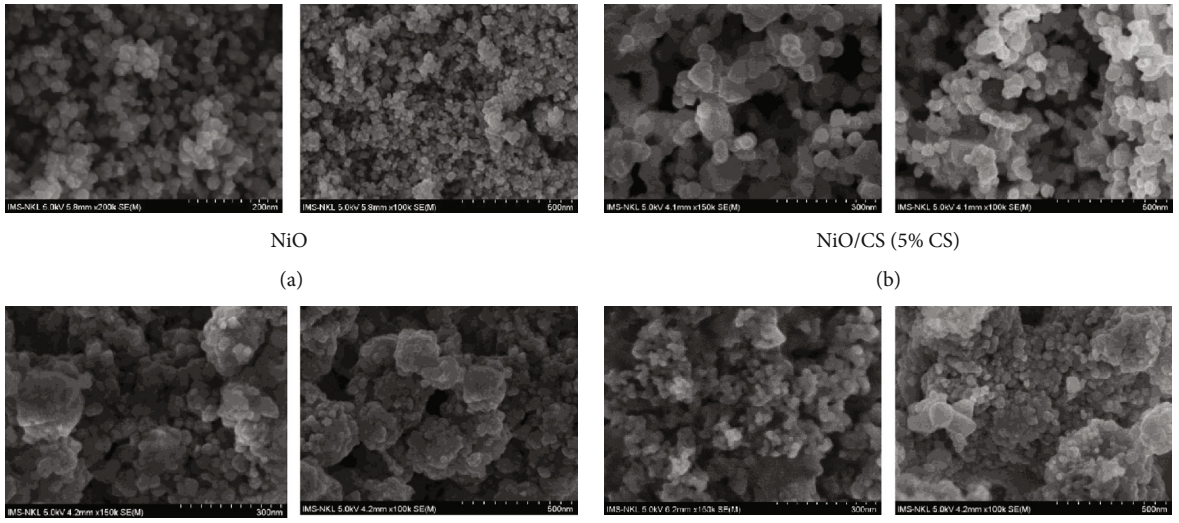


Figure 3: FESEM images of NiO NPs (a) and NiO/CS nanocomposites with different chitosan contents: (b) 5%, (c) 10%, and (d) 20%.

2.2. Preparations of NiO NPs and NiO/CS Nanocomposites. The NiO NPs were prepared using an ultrasound-assisted coprecipitation method. 50 ml of 0.1 M nickel nitrate solution in deionized water was mixed with 50 ml of mangosteen peel extract. The pH of the mixture was controlled between 8 and 9 by adding slowly dropwise 25-28% NH_3 solution. The reaction mixture was then stirred at room temperature with ultrasonic waves (500 W, 20 kHz) for 1 h. The nickel-ellagate complex, which was obtained by centrifugation of the reaction mixture at 7000 rpm for 20 min, was washed several times with deionized water followed by drying at 40°C for 8 h. Finally, NiO NPs were obtained by heating this powder at 450°C.

The method of Bhatt et al. [9] was used to prepare NiO/CS nanocomposites. First, 0.5 g of chitosan was dissolved in 50 ml of acetic acid followed by sonication for 6 h to obtain a solution of 1% chitosan/acetic acid solution. NiO NPs were added to the chitosan solution, and the mixture was sonicated for 1 h. The NiO/CS product was dried in glass Petri dishes in an oven at 60°C for 24 h. The effect of the chitosan mass ratio was evaluated by varying the percentage of mass of chitosan in the sample (5%, 10%, and 20%). Figure 1 schematically shows the process used to prepare the NiO/CS nanocomposites.

2.3. Characterization. The NiO/CS samples were analyzed by X-ray diffraction (XRD) using a P'Pret Pro-PANalytical X-

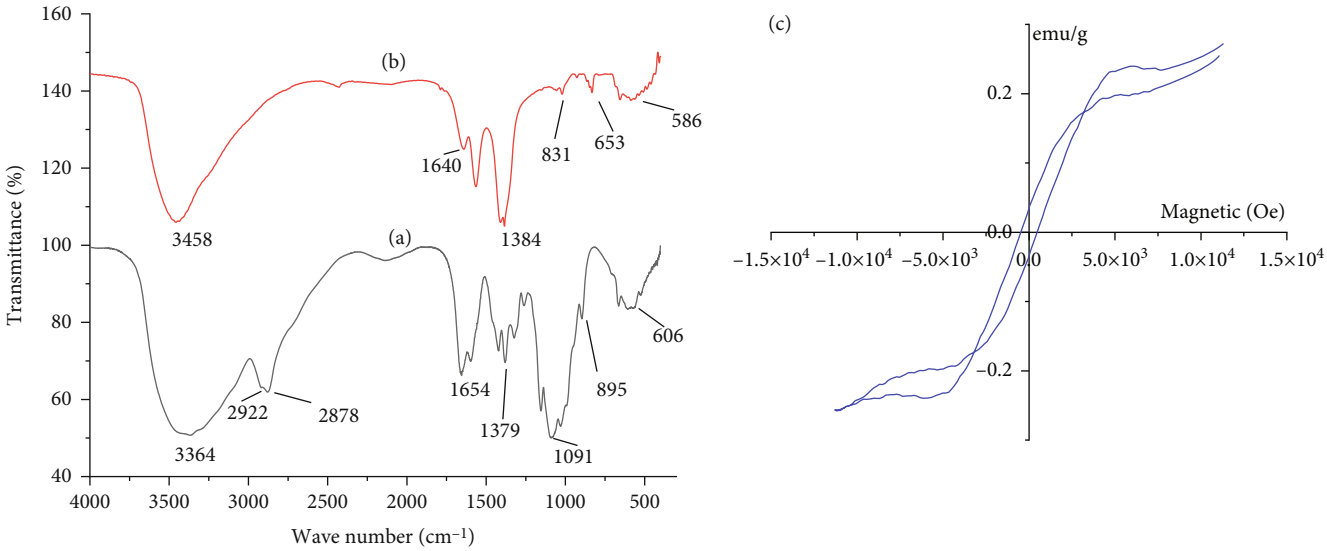


FIGURE 4: FTIR spectra of chitosan (a) and the NiO/CS nanocomposite containing 10% chitosan (b) containing 10% chitosan; M-H curves of NiO/CS (c).

ray diffractometer operating at 1.8 kW (40 mA/45 kV) with CuKα ($\lambda = 1.5406\,\text{Å}$) radiation. The Fourier-transform infrared (FTIR) spectra were recorded using the KBr pellet on a Bruker FTIR spectrometer.

The sizes and morphologies of the NiO NPs and NiO/CS nanocomposites were evaluated by field-emission scanning electron microscopy (FESEM; Hitachi S-4800), transmission electron microscopy (TEM; TEM-JEM1010), and dynamic light scattering (DLS; Malvern instruments). The voltage used for TEM imaging is 80 kV. The zeta potentials of the samples were recorded using a Malvern Zetasizer Nano Z instrument. Magnetic characteristics were observed on the magnet B-10 vibrating sample magnetometer (VSM) instrument at a temperature of 25°C. The NPs were dispersed in deionized water at a concentration of 1 mg/mL concentration to measure the zeta potential.

2.4. Analysis of the Antibacterial Activity of the NiO/CS Nanocomposites. The agar well diffusion method was used to evaluate the antibacterial activity of the NiO/CS compound against Gram-positive *Saccharomyces cerevisiae*, *Bacillus subtilis* (ATCC 9/58) and Gram-negative bacteria (*Escherichia coli* ATCC 25922) [29]. The medium supplemented with substances such as yeast extract, meat extract, glucose, peptone, and some mineral salts was used as a source of nutrients for microbial culture. Nutrient agar plates were prepared by dissolving 37.0 g of nutrient agar media in 1000 mL of distilled water followed by autoclaving at 121°C/15 pounds of pressure for 20 min. After sterilization, the nutrient agar medium was poured into sterile Petri dishes and allowed to solidify. The mature broth cultures of individual pathogenic bacterial strains in the nutrient broth were spread on all surfaces of the agar plates using a sterilized L-shaped glass rod. The antibacterial activity of the reference chitosan sample was also evaluated.

The antibacterial activity assay was carried out as follows: chitosan and NiO/CS nanocomposites were dissolved in 1 ml of dimethyl sulfoxide (DMSO; 10%) to obtain 200 μg/mL solution. Using a sterile steel cork borer, wells with diameters of 5 ± 1 mm were made in each Petri plate under aseptic conditions. Subsequently, 100 μL of CS or NiO/CS was dispersed in 10% DMSO solution, 100 μL standard antibiotic ampicillin (1 mg/mL) was used as a positive control and control into the well. The plates were incubated at 37° C for 24 h. After the incubation period, the zone of inhibition around the well was measured using geometric Vernier calipers.

The test materials (CS, NiO/CS) were sprinkled on the plates to assess the mortality of bacteria in the culture medium. The antibacterial activity tests were carried out in triplicate to determine the antibacterial activity of the NiO NPs.

Minimum inhibitory concentration (MIC) tests of NiO/CS were prepared by the method of Magaña et al. [30]. NiO/CS powders were added to an agar suspension with concentration (3, 2, 1, 0, 5, and 0,3 mg/ml) and cooled until the formation of a gel. The plates were incubated at 37°C/24 h. After that, the MIC of NiO/CS was determined by the naked eye, and the MIC was the lowest concentration of NiO/CS that completely inhibits visible growth.

3. Results and Discussion

3.1. Characterization of the NiO/CS Nanocomposite. Figure 2 shows the XRD patterns of the NiO NPs and NiO/CS nanocomposites synthesized from nickel (II) nitrate hexahydrate and mangosteen peel extract using the ultrasound-assisted coprecipitation method. The diffraction peaks observed at 37.4876°, 44.4894°, and 65.6974° in Figure 2 (1) and at 37.4911°, 44.5036°, and 65.7198° in Figure 2 (2-4) correspond to the planes (111), (200) (200), and (220) planes of the cubic (fcc) structure of NiO, in agreement with previous reports [1, 2, 9, 15]. The peaks at 44.4911° and 51.5036° can

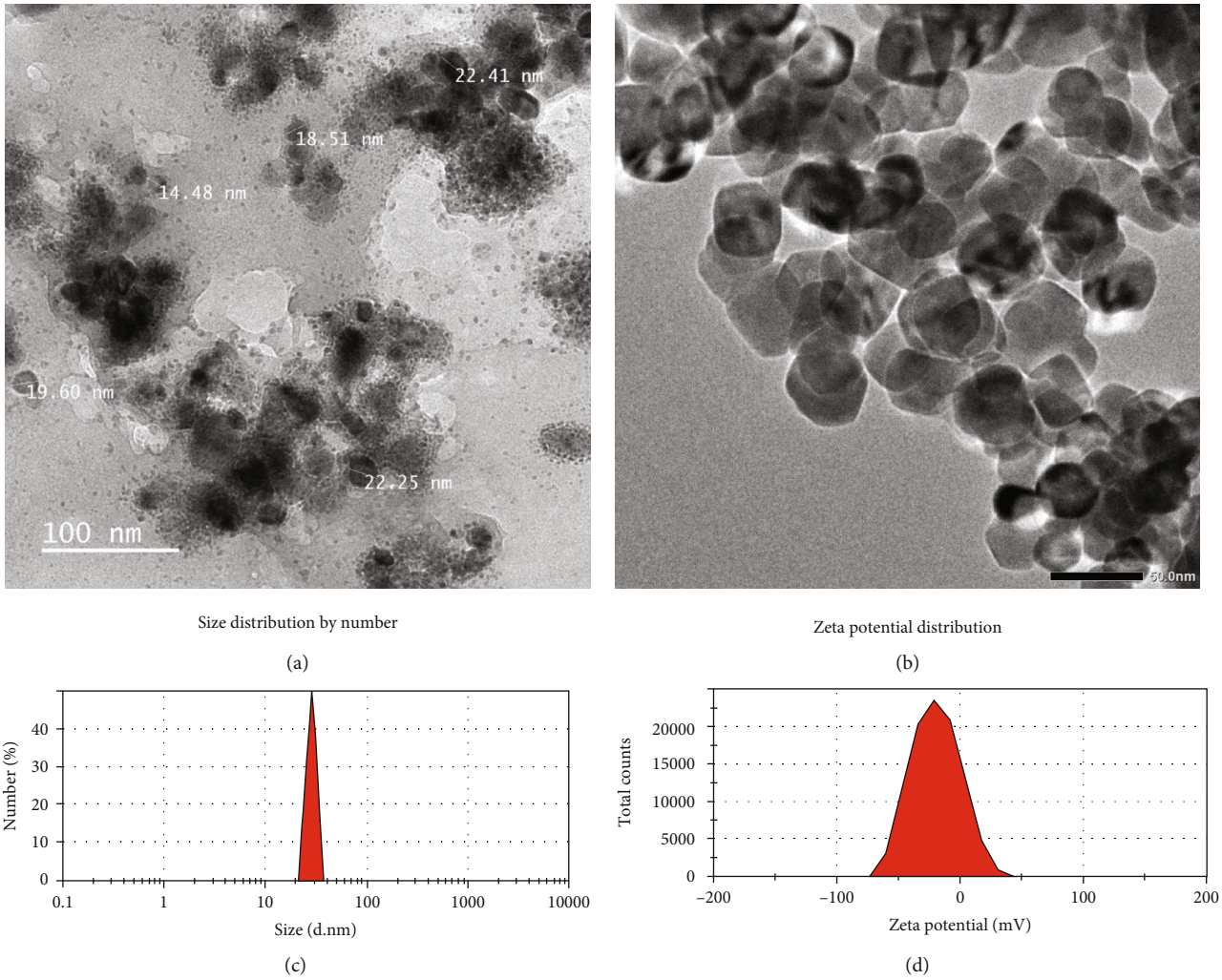


Figure 5: TEM (a) and HR-TEM (b) images of NiO/CS (10% chitosan); (c) particle size distribution and (d) zeta potential distribution of the NiO/CS nanocomposite.

be attributed to the (111) and (200) crystal planes of the fcc structure of metallic nickel NPs [2, 15].

Additional diffraction peaks at approximately 10° and 20.9° in Figure 2 (3-4) indicate the existence of chitosan in the surface nanocomposite (ICSD file no. 98-015-4604) [9]. The crystal size of the NiO NPs was calculated as 14.6 nm using the Debye–Scherrer formula. The FESEM results of the surface characterization and morphology study are shown in Figure 3. The spherical particles are the NiO NPs, whereas the nanofibers are chitosan. The NiO NPs were clearly distributed on chitosan, and most of the chitosan surface was coated with NiO NPs. The chitosan content affected the distribution of NiO NPs on the surface of the chitosan and the surface morphology. The NiO/CS nanocomposite containing 5% chitosan (Figure 3(b)) exhibited a porous morphology with voids between groups of NiO/CS NPs. When the chitosan content increased, the number of voids gradually decreased because the chitosan created a membrane system that enclosed the NiO NPs, which were arranged more closely together (Figures 3(c) and 4(d)). Based on the morphological evaluation (Figure 3), we selected the NiO/CS material containing 10% chitosan for further evaluation because this sample exhibited uniformly distributed NiO NPs on the chitosan surface. Figures 4(a) and 4(b) show the FTIR spectrum of the NiO/CS nanocomposite containing 10% chitosan. Magnetic characteristics of NiO/CS nanocomposite (10%CS) were measured by vibrating sample magnetometer. The particle size was evaluated by TEM and DLS (Figure 5).

The FTIR spectra of all samples show adsorption peaks around 3364 cm^{-1} and 3458 cm^{-1}, which correspond to the OH group and the stretching vibration of free $-NH_2$. The peak at 1643 cm^{-1} can be attributed to the H–O bending mode of water molecules (NiO/CS). The FTIR spectrum of chitosan (spectrum 1 in Figure 4) exhibits the characteristic peak of the β(1-4) glycosidic band in the polysaccharide unit at 1155 cm^{-1}, while the peak at 1091 cm^{-1} indicates the stretching vibration of C–O–C in the glucose circle. The FTIR spectrum of NiO/CS (spectrum 2 in Figure 4) shows the prominent peaks of chitosan at 1598 and 1384 cm^{-1}, which correspond to the NH_2 bending vibration and N–N vibration, respectively [29]. However, these peaks were

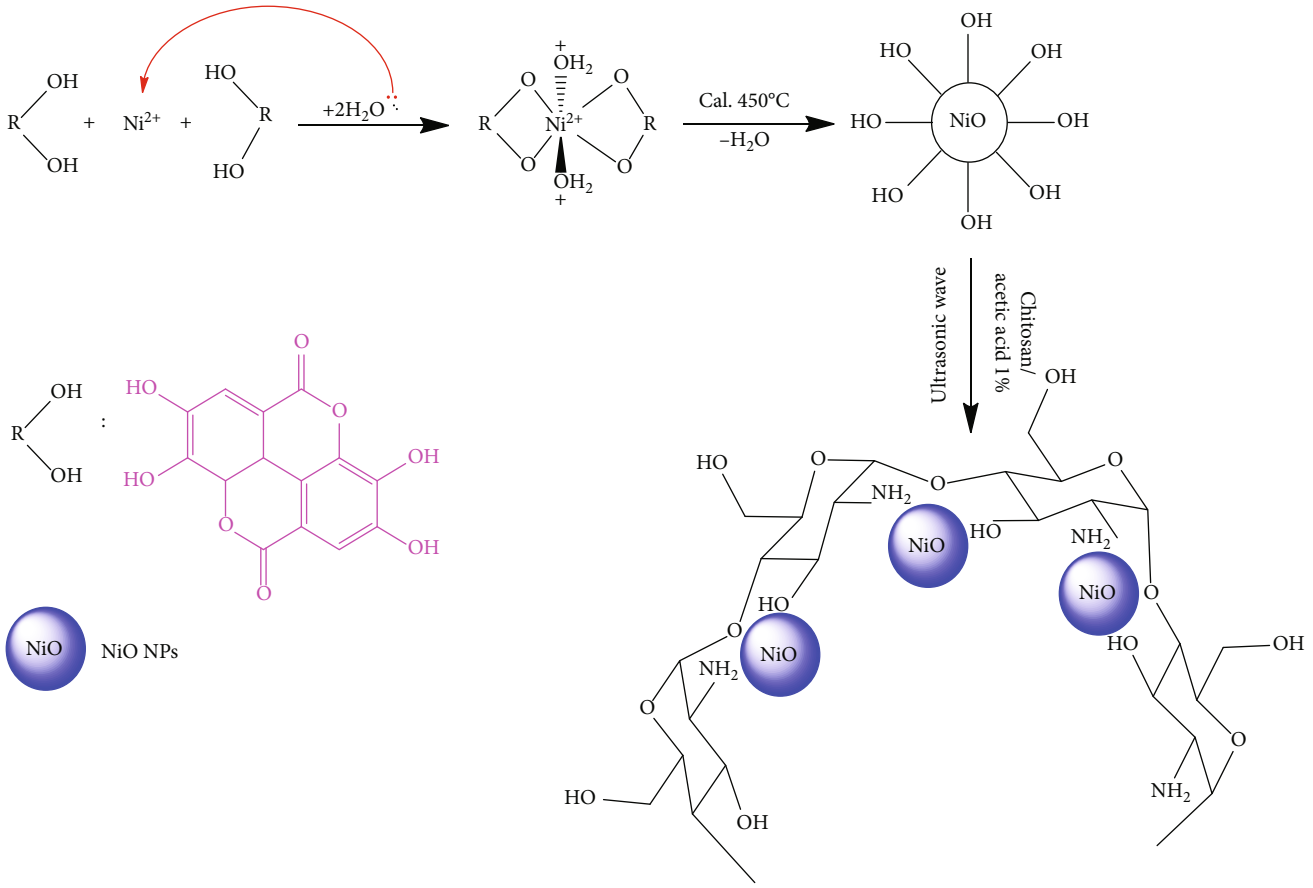


Figure 6: Reaction mechanism for the formation of the NiO/CS nanocomposite.

absent in the NiO/CS spectrum, which shows strong absorption in the fingerprint range at 831, 653, and 586 cm^{-1}, indicating the presence of the Ni–O bond in bare NiO [15, 31].

Characteristics such as coercive field (Hc) and initial susceptibility (χi) are obtained from the magnetization curve. Magnetic saturation is obtained by extrapolating the infinite value of the external magnetic field. For the sample of NiO/CS composite (10% content of CS), this value is about 0.27 emu/g. A previous study by Ghosh et al. [32] reported a similar result of the magnetization curve, with a magnetization value of 0.22 emu/g. Magnetization also contributes to increasing the bactericidal activity of NiO/CS composite materials under the influence of magnetic fields.

The sizes of the spherical NiO NPs distributed on chitosan ranged from 14 to 23 nm (Figures 5(a) and 5(b)). The hydrodynamic sizes of the NiO NPs and NiO/CS nanocomposites in aqueous suspensions were determined by DLS (Figures 5(c) and 5(d)). As shown in Figure 5(c), the NiO/CS nanocomposite exhibited a uniform particle size distribution with an average hydrodynamic diameter of 28 nm, which is reasonably consistent with the FESEM and TEM results. As shown in Figure 5(d), the zeta potential of the NiO/CS nanocomposite containing 10% chitosan was −1.9 mV. The surfaces of the matrix and the composites are positively charged due to the macromolecular NH_3^+ groups in the glucosamine species of chitosan. Upon the incorporation of NiO NPs, the OH group on the NiO surface interacts with the NH^{3+} group to reduce the zeta potential of the NiO/CS composite. This change in zeta potential would alter the interaction of the nanocomposite with Gram-positive and Gram-negative bacteria cells [5, 33]. Figure 6 shows the reaction mechanism for the NiO/CS nanocomposite formation.

3.2. Antibacterial Activity. Figures 7(a)–7(c) show images of the Petri dishes containing chitosan and the NiO/CS nanocomposite inoculated with the three tested microorganisms. These images show the formation of clear zones (nonbacterial zones) around NiO/CS on the Petri dishes inoculated with *B. subtilis*, *S. cerevisiae*, and *E. coli*. Among the microorganisms, the inhibition effect of NiO/CS was strongest for *B. subtilis*. The sizes of the zones of inhibition observed in Figure 7 are listed in Table 1.

NiO NPs interact with microbial cell membranes and bind to mesosomes. These interactions disrupt DNA replication, cell division, and cellular respiration, causing the surface area of the bacterial cell to expand [34]. Some previous publications [26, 35] have shown the good

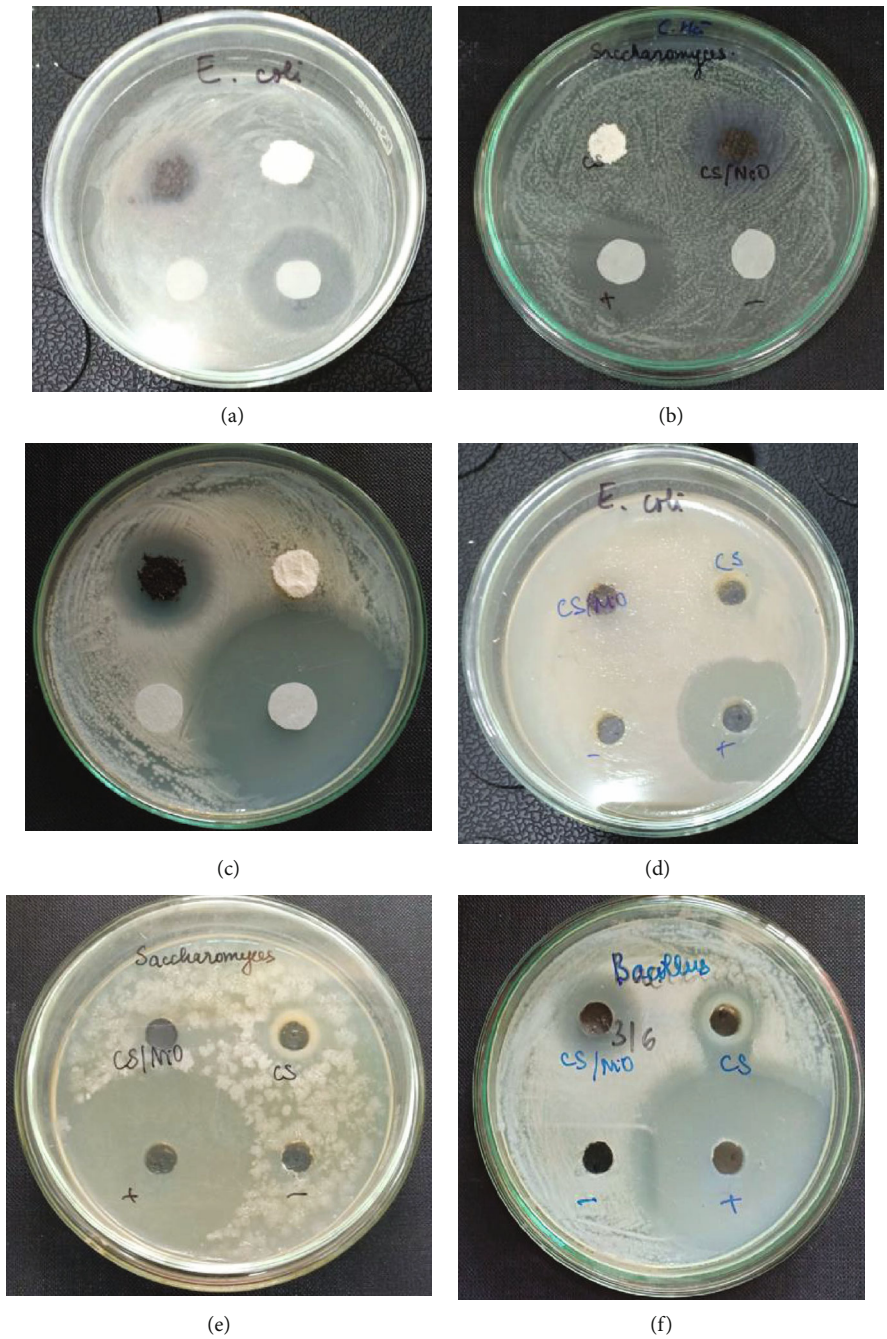


Figure 7: Images showing the antibacterial activities of chitosan and the NiO/CS nanocomposites against pathogenic bacteria: E. coli (a, d), S. cerevisiae (b, e), and B. subtilis (c, f).

Table 1: Antibacterial activity of chitosan and NiO/CS against selected pathogenic bacterial strains.

Sample	Treatment	Zone of inhibition (mm)		
		E. coli (mean ± SE)	*B. subtilis* (mean ± SE)	*S. cerevisiae* (mean ± SE)
CS	Powder	—	2 ± 0.15	—
CS	Solution	8.10 ± 0.15	7.02 ± 0.17	13.30 ± 0.12
NiO/CS	Powder	8.50 ± 0.06	13.23 ± 0.15	15.27 ± 0.15
NiO/CS	Solution	3.33 ± 0.09	10.23 ± 0.12	5.10 ± 0.23

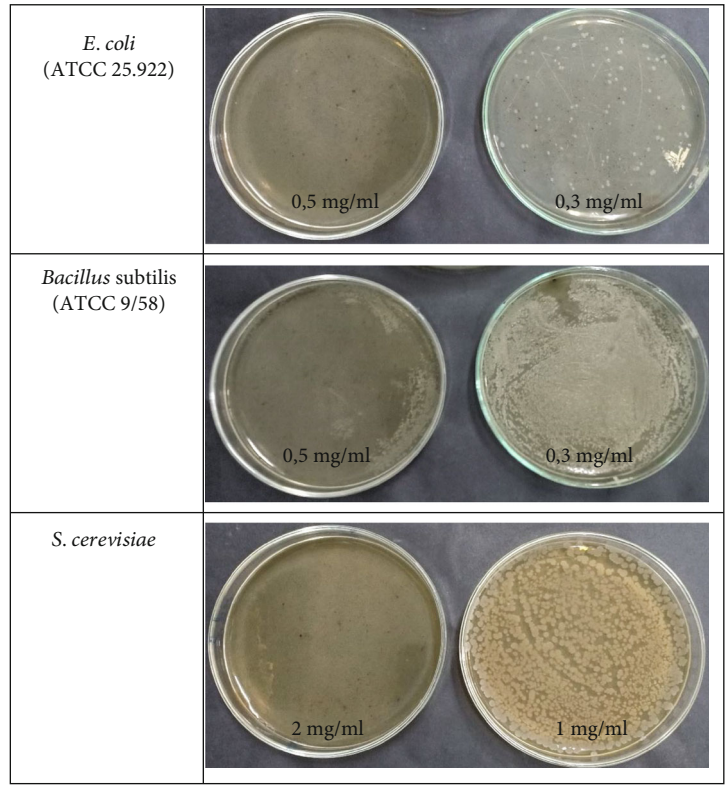


Figure 8: Images showing the antibacterial activities of NiO/CS with different concentration.

Table 2: Comparing antibacterial activity of resultant material with earlier public.

Materials	Conc. (μg/mL)	Synthesis method	Size (nm)	Antibacterial activity (mm)			Ref.
				E. coli	*B. subtilis*	*S. cerevisiae*	
NiO	10.000	*Raphanus sativus* extract	13	4.175	2.176	—	[39]
NiO	10	Onion extract	75	10	—	—	[40]
NiO	—	Hydrothermal method	75	10	—	16	[41]
S,N-GQDs/NiO	—		—	16	—	19	
NiO	2.000	*Populus ciliata* leaves extract	44	13.2	15.2	—	[42]
	4.000			18.3	24.1	—	
	8.000			22.1	28.1	—	
NiO	50	*Clitoria ternatea* flower extract	13	15	—	—	[43]
	100			17	—	—	
	200			22	—	—	
NiO/CS	200	Mangosteen peel extract	28	3.33	10.23	5.10	Present work

antibacterial capacity of chitosan against both Gram-negative and Gram-positive bacteria in acidic media. Therefore, NiO/CS exhibited stronger bacteriostatic activity against *B. subtilis* than against *E. coli*.

Like NiO NPs, NiO/CS releases Ni^{2+} ions on the chitosan surface, the negatively charged NiO/CS nanocomposite interacting with the positively charged bacterial cell membrane is drawn back and forth, and the metal ions diffuse into it. The presence of metal ions on the bacterial surface is represented by thiol (–SH) groups, metabolized from proteins. Bacterial death is caused by the diffusion of nutrients carried by proteins formed across the bacterial cell membrane and the inactivation of proteins activated by NPs, reducing cell permeability. NPs immediately react with pathogenic bacteria to destroy membrane integrity, resulting in bacterial cell death [36–38].

The results in Table 1 show that the bactericidal effect of powdered NiO/CS has been significantly improved compared to CS, especially with Gram-positive bacteria (*B. subtilis*). However, this result also observed a slight decrease in the antibacterial diameter of the solution NiO/CS sample. This can be attributed to the poor solubility of NiO/CS.

Figure 8 shows images of the Petri dishes, which were the MIC test results of the NiO/CS nanocomposites. The MIC

values against *E. coli*, *B. subtilis*, and *S. cerevisiae* of NiO/CS nanocomposite were 0.3, 0.3, and 1 mg/ml, respectively.

The antibacterial activity of NiO/CS in this study is compared with some similar materials previously published as shown in Table 2. The results show that NiO/CS is able to compared with some grades of NiO NPs were synthesized by another green method.

4. Conclusion

NiO/CS nanocomposites were successfully synthesized using mangosteen (*G. mangostana* L.) peel extract via an ultrasound-assisted route. The intense (200) XRD peak revealed the formation of NiO NPs with cubic structures. The results of TEM and DLS analysis have demonstrated that the spherical NiO NPs are uniformly distributed on chitosan. FTIR spectroscopy confirmed the formation of NiO NPs based on the Ni–O stretching vibration. The antibacterial activity of NiO/CS nanocomposites against Gram-negative *Escherichia coli* and Gram-positive *Saccharomyces cerevisiae*, *Bacillus subtilis* bacteria strains were evaluated. NiO/CS eliminated both bacterial cells and fungal (mold) cells adjacent to the nanocomposite, with the strongest inhibition observed for *B. subtilis*. The results suggest that the prepared NiO/CS composite is appropriate for pharmaceutical applications.

Data Availability

The data used to support the findings of this study are available from the corresponding author Nguyen Thi Huong. Please contact us at nguyenhuong0916@gmail.com.

Conflicts of Interest

The authors declare that there are no conflicts of interest regarding the publication of this paper.

Authors' Contributions

T.H.N conceived of the present idea. N.S.N and T.M.H.P introduced related scientific content. T.H.N and N.S.N designed and planned the experiments. T.N.D, H.N.P, and T.H.N carried out the experiments and gathered results. T.H.N and T.T.L interpreted the results. T.H.N took the lead in writing the manuscript with input from all authors. All authors have read and agreed to the published version of the manuscript.

References

[1] K. Karthik, M. Shashank, V. Revathi, and T. Tatarchuk, "Facile microwave-assisted green synthesis of NiO nanoparticles fromAndrographis paniculataleaf extract and evaluation of their photocatalytic and anticancer activities," *Molecular Crystals and Liquid Crystals*, vol. 673, no. 1, pp. 70–80, 2018.

[2] G. Zhang, Y. Chen, B. Qu et al., "Synthesis of mesoporous NiO nanospheres as anode materials for lithium ion batteries," *Electrochimica Acta*, vol. 80, pp. 140–147, 2012.

[3] M. Fouladgar, H. Karimi-Maleh, and V. K. Gupta, "Highly sensitive voltammetric sensor based on NiO nanoparticle room temperature ionic liquid modified carbon paste electrode for levodopa analysis," *Journal of Molecular Liquids*, vol. 208, pp. 78–83, 2015.

[4] W. W. Andualem, F. K. Sabir, E. T. Mohammed, H. H. Belay, and B. A. Gonfa, "Synthesis of copper oxide nanoparticles using plant leaf extract of Catha edulis and its antibacterial activity," *Journal of Nanotechnology*, vol. 2020, Article ID 2932434, 10 pages, 2020.

[5] V. M. Thanh, N. T. Huong, D. T. Nam, N. D. T. Dung, T. Le Van, and M.-T. Nguyen-Le, "Synthesis of ternary Fe_3O_4/ZnO/chitosan magnetic nanoparticles via an ultrasound-assisted coprecipitation process for antibacterial applications," *Journal of Nanomaterials*, vol. 2020, Article ID 8875471, 9 pages, 2020.

[6] Z. Chen, P. Liu, A. Zare, A. Karimipour, A. Abdollahi, and I. Tlili, "Evaluation of thermal conductivity of deionized water containing SDS-coated NiO nanoparticles under the influences of constant and alternative varied magnetic fields," *Powder Technology*, vol. 367, pp. 143–156, 2020.

[7] A. Nel, T. Xia, L. Mädler, and N. Li, "Toxic potential of materials at the nanolevel," *Science*, vol. 311, no. 5761, pp. 622–627, 2006.

[8] B. Varghese, M. V. Reddy, Z. Yanwu, C. S. Lit, and T. C. Hoong, "Fabrication of NiO nanowall electrodes for high performance lithium ion battery," *Chemistry of Materials*, vol. 20, no. 10, pp. 3360–3367, 2008.

[9] A. S. Bhatt, D. K. Bhat, M. S. Santosh, and C. W. Tai, "Chitosan/NiO nanocomposites: a potential new dielectric material," *Journal of Materials Chemistry*, vol. 21, no. 35, pp. 13490–13497, 2011.

[10] P. M. Ponnusamy, S. Agilan, N. Muthukumarasamy et al., "Structural, optical and magnetic properties of undoped NiO and Fe-doped NiO nanoparticles synthesized by wet-chemical process," *Materials Characterization*, vol. 114, pp. 166–171, 2016.

[11] N. N. M. Zorkipli, N. H. M. Kaus, and A. A. Mohamad, "Synthesis of NiO nanoparticles through sol-gel method," *Procedia Chemistry*, vol. 19, pp. 626–631, 2016.

[12] S. Sunkar and C. V. Nachiyar, "Biogenesis of antibacterial silver nanoparticles using the endophytic bacterium *Bacillus cereus* isolated from *Garcinia xanthochymus*," *Asian Pacific Journal of Tropical Biomedicine*, vol. 2, no. 12, pp. 953–959, 2012.

[13] N. Vigneshwaran, N. M. Ashtaputre, P. V. Varadarajan, R. P. Nachane, K. M. Paralikar, and R. H. Balasubramanya, "Biological synthesis of silver nanoparticles using the fungus *Aspergillus flavus*," *Materials Letters*, vol. 61, no. 6, pp. 1413–1418, 2007.

[14] S. Saleem, B. Ahmed, M. S. Khan, M. Al-Shaeri, and J. Musarrat, "Inhibition of growth and biofilm formation of clinical bacterial isolates by NiO nanoparticles synthesized from *Eucalyptus globulus* plants," *Microbial Pathogenesis*, vol. 111, pp. 375–387, 2017.

[15] A. A. Olajire and A. A. Mohammed, "Green synthesis of nickel oxide nanoparticles and studies of their photocatalytic activity in degradation of polyethylene films," *Advanced Powder Technology*, vol. 31, no. 1, pp. 211–218, 2020.

[16] M. N. Nadagouda and R. S. Varma, "Green and controlled synthesis of gold and platinum nanomaterials using vitamin B2:

density-assisted self-assembly of nanospheres, wires and rods," *Green Chemistry*, vol. 8, no. 6, pp. 516–518, 2006.

[17] P. Karthiga, "Preparation of silver nanoparticles by Garcinia mangostana stem extract and investigation of the antimicrobial properties," *Biotechnology Research and Innovation*, vol. 2, no. 1, pp. 30–36, 2018.

[18] M. Aminuzzaman, L. P. Ying, W.-S. Goh, and A. Watanabe, "Green synthesis of zinc oxide nanoparticles using aqueous extract of Garcinia mangostana fruit pericarp and their photocatalytic activity," *Bulletin of Materials Science*, vol. 41, no. 2, 2018.

[19] W. Pothitirat, M. T. Chomnawang, R. Supabphol, and W. Gritsanapan, "Comparison of bioactive compounds content, free radical scavenging and anti- acne inducing bacteria activities of extracts from the mangosteen fruit rind at two stages of maturity," *Fitoterapia*, vol. 80, no. 7, pp. 442–447, 2009.

[20] W. Suttirak and S. Manurakchinakorn, "In vitro antioxidant properties of mangosteen peel extract," *Journal of Food Science and Technology*, vol. 51, no. 12, pp. 3546–3558, 2014.

[21] S. Tjahjani, W. Widowati, K. Khiong, A. Suhendra, and R. Tjokropranoto, "Antioxidant properties of *Garcinia mangostana* L (mangosteen) rind," *Procedia Chemistry*, vol. 13, pp. 198–203, 2014.

[22] L. Adriani, T. Widjastuti, R. R. Nurdianti, and R. Wiradimadja, "Effects of Mangosteen Peel Extract (Garcinia mangostana L.) on Blood Lipid of Sentul Chicken Growth Phase," in *3rd International Conference of Integrated Intellectual Community (ICONIC)*, Hannover, Germany, 2018.

[23] S. Melia, D. Novia, I. Juliyarsi, and E. Purwati, "The characteristics of the pericarp of Garcinia mangostana (mangosteen) extract as natural antioxidants in rendang," *IOP Conference Series: Earth and Environmental Science*, vol. 287, no. 1, article 012028, 2019.

[24] W. Tachaboonyakiat, *Chitosan Based Biomaterials Volume 2*, J. A. Jennings and J. D. Bumgardner, Eds., Woodhead Publishing, 2017.

[25] Z. Jia, D. Shen, and W. Xu, "Synthesis and antibacterial activities of quaternary ammonium salt of chitosan," *Carbohydrate Research*, vol. 333, no. 1, pp. 1–6, 2001.

[26] H. K. No, N. Young Park, S. Ho Lee, and S. P. Meyers, "Antibacterial activity of chitosans and chitosan oligomers with different molecular weights," *International Journal of Food Microbiology*, vol. 74, no. 1-2, pp. 65–72, 2002.

[27] W. Sun, L. Chen, S. Meng et al., "Synthesis of NiO nanospheres with ultrasonic method for supercapacitors," *Materials Science in Semiconductor Processing*, vol. 17, pp. 129–133, 2014.

[28] V. Ramasamy Raja, D. Rani Rosaline, A. Suganthi, and M. Rajarajan, "Ultrasonic assisted synthesis with enhanced visible-light photocatalytic activity of NiO/Ag_3VO_4 nanocomposite and its antibacterial activity," *Ultrasonics Sonochemistry*, vol. 44, pp. 73–85, 2018.

[29] H. Abdolmohammad-Zadeh, Z. Ayazi, and Z. Naghdi, "Nickel oxide/chitosan nano-composite as a magnetic adsorbent for pre- concentration of Zn(II) ions," *Journal of Magnetism and Magnetic Materials*, vol. 488, article 165311, 2019.

[30] S. M. Magaña, P. Quintana, D. H. Aguilar et al., "Antibacterial activity of montmorillonites modified with silver," *Journal of Molecular Catalysis A: Chemical*, vol. 281, no. 1-2, pp. 192–199, 2008.

[31] K. Lingaraju, H. Raja Naika, H. Nagabhushana, K. Jayanna, S. Devaraja, and G. Nagaraju, "Biosynthesis of nickel oxide nanoparticles from *Euphorbia heterophylla* (L.) and their biological application," *Arabian Journal of Chemistry*, vol. 13, no. 3, pp. 4712–4719, 2020.

[32] M. Ghosh, K. Biswas, A. Sundaresan, and C. N. R. Rao, "MnO and NiO nanoparticles: synthesis and magnetic properties," *Journal of Materials Chemistry*, vol. 16, no. 1, pp. 106–111, 2006.

[33] L. Qi, Z. Xu, X. Jiang, C. Hu, and X. Zou, "Preparation and antibacterial activity of chitosan nanoparticles," *Carbohydrate Research*, vol. 339, no. 16, pp. 2693–2700, 2004.

[34] A. M. Ramadan, "Structural and biological aspects of copper (II) complexes with 2-methyl-3-amino-(3 *H*)-quinazolin-4-one," *Journal of Inorganic Biochemistry*, vol. 65, no. 3, pp. 183–189, 1997.

[35] Z. Li, X. P. Zhuang, X. F. Liu, Y. L. Guan, and K. D. Yao, "Study on antibacterial O -carboxymethylated chitosan/cellulose blend film from LiCl/N, N-dimethylacetamide solution," *Polymer*, vol. 43, no. 4, pp. 1541–1547, 2002.

[36] M. Soltani Nejad, M. Khatami, and B. G. H. Shahidi, "Streptomyces somaliensis mediated green synthesis of silver nanoparticles," *Nanomedicine Journal*, vol. 2, pp. 233–238, 2015.

[37] V. Vinotha, A. Iswarya, R. Thaya et al., "Synthesis of ZnO nanoparticles using insulin-rich leaf extract: anti-diabetic, antibiofilm and anti-oxidant properties," *Journal of Photochemistry and Photobiology B: Biology*, vol. 197, article 111541, 2019.

[38] K. Kannan, D. Radhika, M. P. Nikolova, K. K. Sadasivuni, H. Mahdizadeh, and U. Verma, "Structural studies of biomediated NiO nanoparticles for photocatalytic and antibacterial activities," *Inorganic Chemistry Communications*, vol. 113, article 107755, 2020.

[39] S. Haq, S. Dildar, M. B. Ali et al., "Antimicrobial and antioxidant properties of biosynthesized of NiO nanoparticles using Raphanus sativus (R. sativus) extract," *Materials Research Express*, vol. 8, no. 5, article 055006, 2021.

[40] M. Nawaz, M. B. Tahir, T. Iqbal et al., "Synthesis, characterization and antibacterial activity of NiO NPs against pathogen," *Inorganic Chemistry Communications*, vol. 122, article 108300, 2020.

[41] S. G. Al-Shawi, N. Andreevna Alekhina, S. Aravindhan et al., "Synthesis of NiO nanoparticles and sulfur, and nitrogen co doped-graphene quantum dots/ NiO nanocomposites for antibacterial application," *Journal of Nanostructures*, vol. 11, pp. 181–188, 2021.

[42] M. Hafeez, R. Shaheen, B. Akram et al., "Green synthesis of nickel oxide nanoparticles using Populus ciliata leaves extract and their potential antibacterial applications," *South African Journal of Chemistry*, vol. 75, 2021.

[43] S. Prabhu, T. Daniel Thangadurai, P. Vijai Bharathy, and P. Kalugasalam, "Synthesis and characterization of nickel oxide nanoparticles using Clitoria ternatea flower extract: photocatalytic dye degradation under sunlight and antibacterial activity applications," *Results in Chemistry*, vol. 4, article 100285, 2022.